16th World Conference on Earthquake, 16WCEE 2017

Santiago Chile, January 9th to 13th 2017

Paper N° 1230

Registration Code: S-XXXXXXXX

EXPERIMENTAL EVALUATION OF SEISMIC PERFORMANCE OF A HYBRID WALLED-FRAME SYSTEM IN THERMAL POWER PLANTS

Yongtao Bai[(1)], and Guoliang Bai[(2)]

[(1)] *Assistant professor, Department of Civil Engineering, Xi'an Jiaotong University, baiyongtao@xjtu.edu.cn*
[(2)] *Professor, School of Civil Engineering, Xi'an University of Architecture and Technology, guoliangbai@126.com*

Abstract

This paper presents a series of experiments on seismic performance of a steel-concrete walled-frame system subjected to incremental earthquakes. Pseudo-dynamic tests were performed on a one-seventh scaled specimen to investigate the that was subjected to the El-Centro NS wave. The tested specimen with steel reinforced concrete (SRC) frame and reinforced concrete (RC) wing-walls was designed for industrial buildings in thermal and nuclear power plants. Due to special requirements from facility installation, beam-column connections were designed with inevitable strong-beam weak-column mechanism, wing walls aim to primarily dissipate hysteretic energy and postpone the damage and collapse the frame. Test results indicates that the specimen demonstrated dual seismic-resisting mechanism under severe earthquakes with PGA=3.0 g which is beyond the code requirement of with the return period 2 % in 50 years. A region of drift concentration was found in the range of 2.40~4.80 m. Various primary story levels of the specimen showed difference in lateral stiffness, which is consistent with the contribution ratios of the cumulative hysteretic energy. The first and second primary stories dissipated most of the input hysteretic energy. This hybrid structural system is anticipated to provide high ductility as industrial buildings in seismic prone regions.

Keywords: Hybrid structures; Seismic performance; Pseudo dynamic tests; Wing walls; Power plants

1. Introduction

Steel-concrete composite structures become more and more popular because they combine the advantages of both materials. During the 1994 Northridge Earthquake [1-3] and 1995 Hyogoken-Nanbu (Kobe) Earthquake [4], a large number of RC and SRC frame buildings experienced severe damages. Moreover, in the 2011 Tohoku Earthquake [5], the Fukushima No. 1 nuclear power plant and thermal power plant buildings constructed by steel-concrete composite frame suffered severe damages and massive loss of casualties. These industrial building structures face failure risks because of large span and story height, split-level floor layout and massive vertical loads. Accordingly, special design is required considering strong-beam weak-column mechanism, discontinuous stiffness over height and high axial force on columns.

SRC columns demonstrated ductile behavior because the core concrete is confined by steel hoops, and the buckling of longitudinal bars is contrarily restrained the encased concrete. On the other hand, RC walled-frames exhibit superior seismic behavior than bare RC frames, since RC wall enhances ductility when improving the deflection pattern at the lower stories of the frame. For the factory buildings in power plants, generators and facilities limit the space to use continuous RC wall systems. The RC wing-wall system is beneficial because it not only effectively avoids the weak-story mechanism by increasing the lateral stiffness, but save the space for non-structural components and facilities. Existing experimental studies on the flexural and shear strengths of RC columns with wing walls [6-9] and RC wing-walled frames [10-13] have been conducted. These studies found that brittle flexural failure was likely to occur at RC columns and shear failure occurred at wing walls, and shear failure of column and wing wall was observed as well. In addition, RC columns with wing walls barely demonstrate ductile behavior under high axial load. The literature review indicates that the study on SRC frame system with RC wing walls is very limited.

Considering the irregular characteristics existing in the main factory buildings of TPPs, seismic behavior of such building structures motivates us to enhance their seismic behavior and ductility. For this purpose, a dual structural system with irregular SRC frame combined with RC wing walls is proposed. This paper presents a series of pseudo-dynamic tests on a large scale walled- frame specimen were conducted for evaluating the seismic performance under incremental seismic actions.

2. Pseudo-Dynamic Test

2.1 Design of specimens

The prototype structure is a factory building in thermal power plants in high seismicity zone of China. As shown in Fig. 1, the overall width, length and height of the building are 58, 122, and 59.5 m, respectively [14]. Note that irregular components and large spans are widely distributed because of facility requirements. The prototype structure was designed by the 8-degree seismic demand and assumed to be located on the type 2 soil site based on China seismic design code. The 8-degree seismic demand specifies that the structure should satisfy seismic demands under three seismic hazard levels, namely, minor earthquake having 63.3% probability in 50 years, moderate earthquake having 10% probability in 50 years, and major earthquake having 2% probability in 50 years. The peak ground acceleration (PGA) of 0.15 g was used for minor earthquake, 0.30 g for moderate earthquake and 0.40 g for major earthquake. Particularly, the moderate and major earthquakes are respectively associated with the design basis earthquake (DBE) and maximum considered earthquake (MCE) in ASCE-7-10 15.

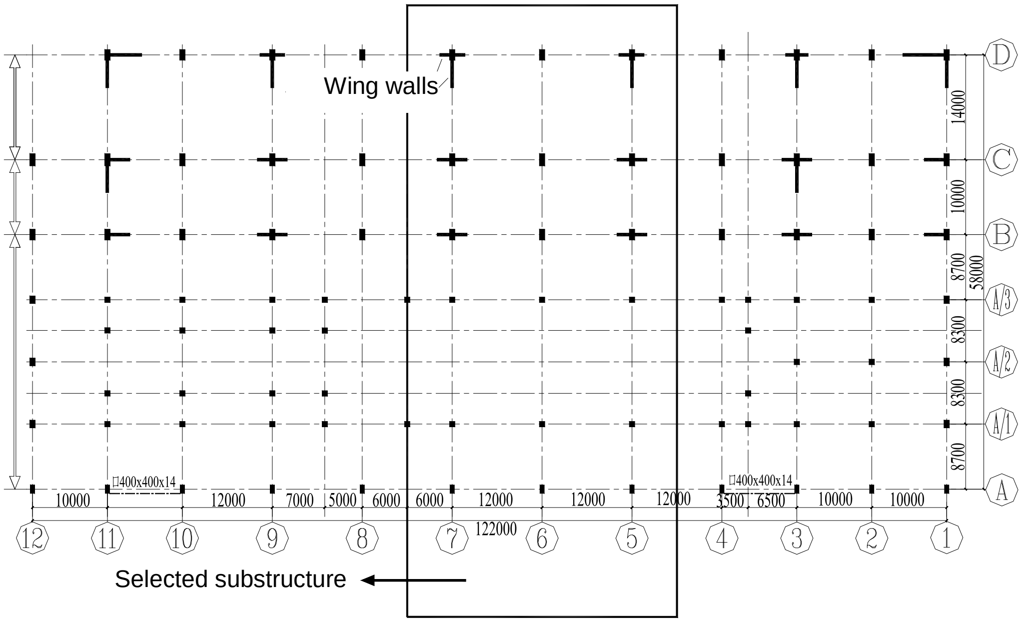

Fig. 1 – Prototype and sub-structure specimen

Due to limitation of the test field and enormous dimension of the prototype structure, a scaled sub-structural specimen was selected, as shown in Fig. 1. Three fundamental scale dimensions of mass M, length L and time T need to be considered as independent scale factors. Then, other scale factors can be obtained by the principle of dimensional analysis. For the structural system in this study, the scale factor for length L was determined as 1/7. In addition, around 1/5 of the vertical additional mass was added on each floor by sand bags to accommodate the limitation in space and enormous vertical loads. Therefore, the mass factor M should further incorporate the effect caused by insufficient vertical loads. Table 1 presents scaled factors of the specimen.

Table 1 – Scale factors of specimen compared to prototype structure

Category	Quantity	Dimension	Procedure	Scale factor
Material	Stress	$[FL^{-2}]$	$S_\sigma = S_E$	1/5
	Strain	[-]	$S_\varepsilon = S_\sigma / S_E$	1/5
	Young's modulus	$[FL^{-2}]$	S_E	1
Geometry	Length	$[L]$	$S_L = L_m / L_p$	1/7
	Displacement	$[L]$	$S_x = S_L$	1/7
	Area	$[L^2]$	$S_A = S_L^2$	1/49
Loads	Concentrated load	$[F]$	S_p	2/490
	Line load	$[FL^{-1}]$	S_q	3/70
	Area load	$[FL^{-2}]$	S_ω	1/5
	Seismic load	$[F]$	$S_F = S_E S_L^2$	1/49
Dynamic characteristics	Mass	$[FL^{-1}T^{2}]$	$S_m = S_\sigma S_L^2$	2/490
	Stiffness	$[FL^{-1}]$	$S_k = S_E S_L$	1/7
	Time	$[T]$	$S_t = [(S_\sigma S_L) / S_E]^{1/2}$	$\sqrt{2/70}$
	Velocity	$[LT^{-1}]$	$S_v = [(S_E S_L) / S_\sigma]^{1/2}$	$\sqrt{5/7}$
	Input acceleration	$[LT^{-2}]$	S_E / S_σ	5/1
	Output	$[LT^{-2}]$	$S_a = S_E / S_\sigma$	5/1

	acceleration			
	Frequency	$[T^{-1}]$	$S_f=[S_E/(S_\sigma S_L)]^{1/2}$	$\sqrt{70/2}$

Fig. 2 illustrates plan dimension, transverse and longitudinal elevation views of the tested specimen with three spans and three bays in longitudinal and transverse directions, respectively. There were three primary story levels located at 0.00, 2.40, and 7.20 meters high. Rectangular SRC columns were used as the interior and exterior columns from alignment B to D, and RC wing walls were arranged within the width and depth of the exterior columns. RC slabs with 50 mm thickness were constructed at each floor. Column bases were fixed by the embedded RC beam foundations.

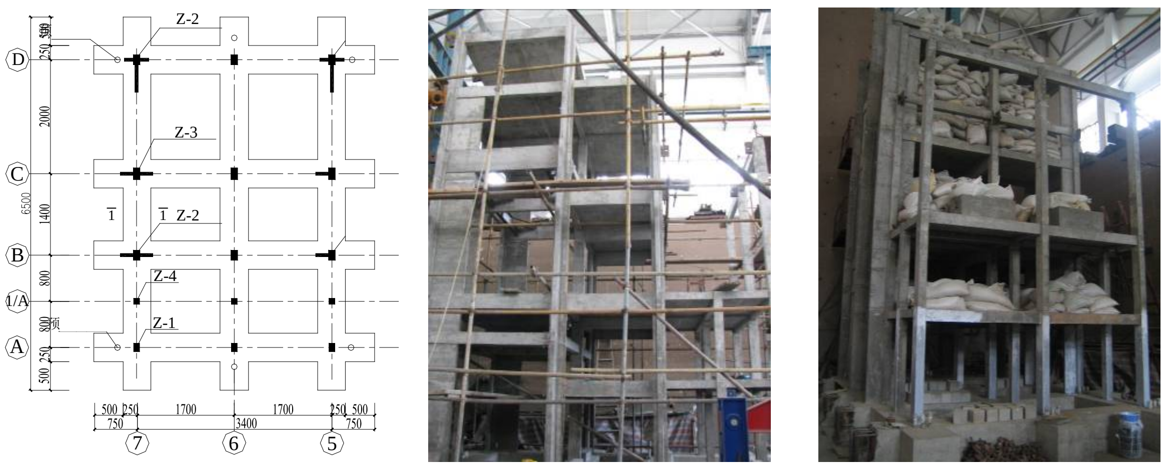

(a) Plan dimension (b) Transverse elevation view (c) Longitudinal elevation view

Fig. 2 –Plan dimension, transverse and longitudinal elevation views of the tested specimen

Fig. 3 shows the sectional properties and steel arrangements of the SRC columns with bi-directional RC wing walls. The RC wing walls was reinforced by lateral and vertical steel bars with boundary reinforcements. The lateral steel bars in wing walls passed through the web of the encased H-shaped W sectional steel in the SRC columns. The Q235 grade steel with the nominal yield strength of 235 MPa was used for the H-shaped W-sectional steel in SRC columns. The average tested yield strengths for the H-shaped steel and steel bars are 340 and 528 MPa, respectively. The C30 grade concrete with the nominal compressive cube strength of 30 MPa was used for the beam foundation and slabs, and C45 grade concrete with the nominal compressive cube strength of 45 MPa was used for the beam and column components. The actual strengths of concrete were tested by the compressive test of concrete cube with 150 mm in width, and the average compressive stress was 30.9 MPa.

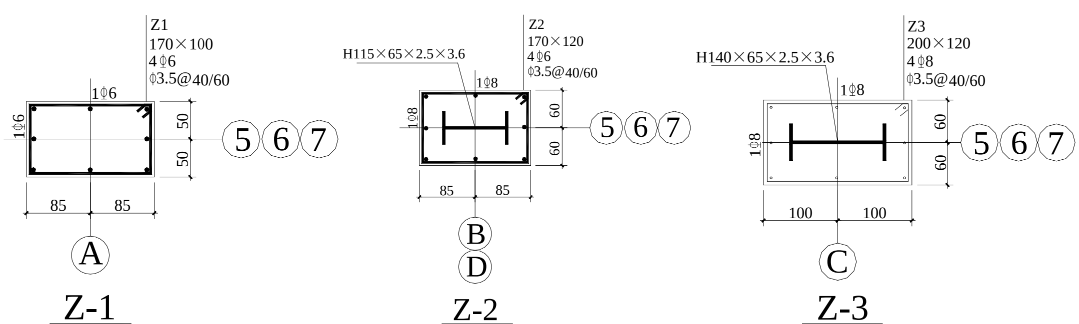

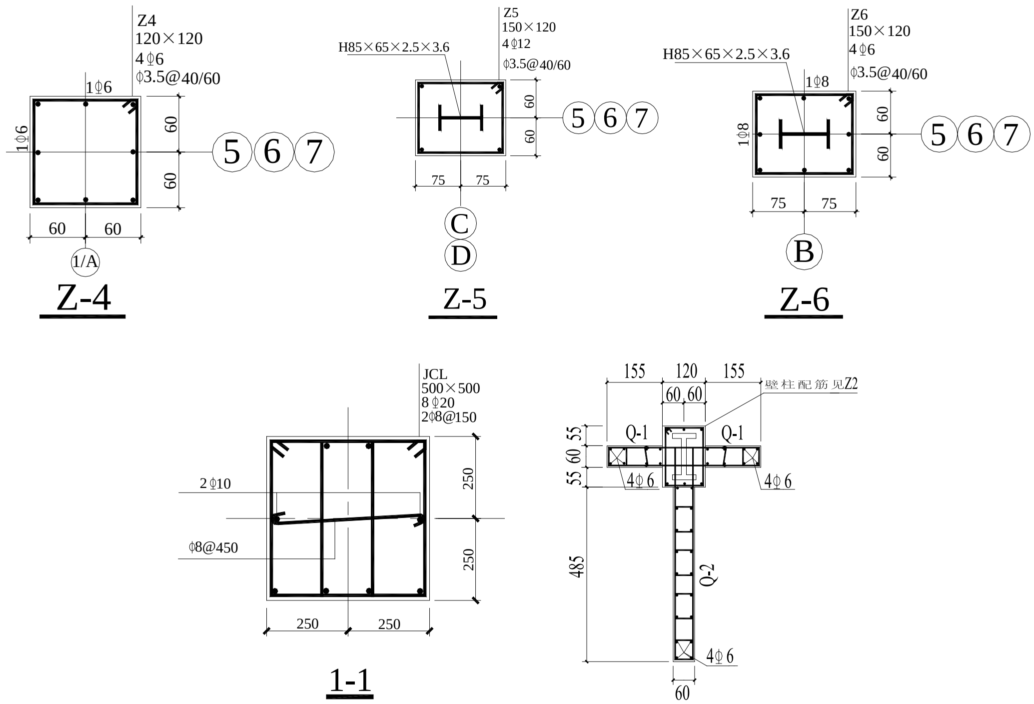

Fig. 3 –Sectional details of the SRC beam-column with RC wing-walls

2.2 Loading protocol

A series of PDTs and subsequent cyclic QSTs were conducted to investigate the seismic behavior and ultimate failure mechanism. In the online PDT procedure, the explicit Newmark-β integration method was adopted to calculate the input force provided by electro-hydraulic actuators. The time increment for each input step was set as 0.01 s to meet the convergence condition. An initial part of the El-Centro (N-S) wave was selected as the input ground motion, and the intensity was incrementally increased to have the peak ground accelerations (PGA) of 100, 250, 500, 1000, 1500, 2000, and 3000 gal for total of seven cases. In specific, 500, 1000 and 2000 indicates the small, moderate and large earthquake in 8-degree seismic zone of China. The scaled input PGA is 1/5 of the original PGA according to the scale factor on acceleration. Fig. 4 shows the selected initial 8 seconds of the El-Centro (N-S) wave with a PGA of 0.50 g which was loaded by 800 quasi-static steps, and subsequent 2 seconds was loaded by 200 steps to simulate free vibration.

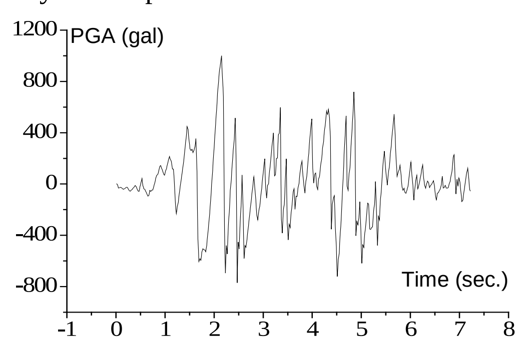

Fig. 4 –Loading actuators, measurement and vertical load

In addition, vertical loads of the prototype structure were added owing to the scale factor of length S_L of 1/7. The scaled vertical load requires the space larger than the floor area of the specimen. This is because that the floor area was scaled by to 1/49 of the prototype structure. Thus, sandbags and steel blocks equivalent to 1/5 of the scaled vertical load were put on the RC slabs at each floor. Fig. 5 shows loading actuators, measurement and vertical load of the specimen.

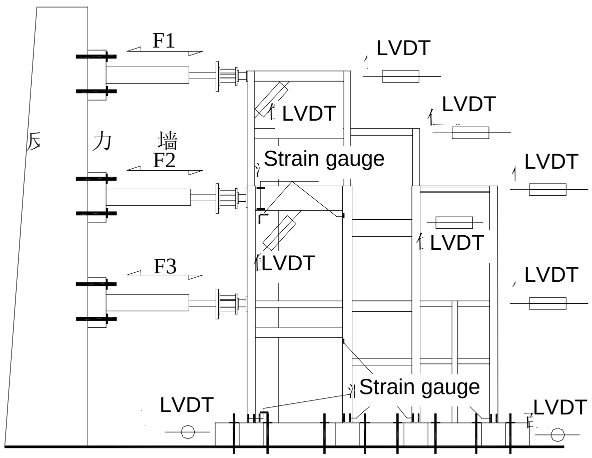

(a) Loading actuators and measurement

(b) Vertical load

Fig. 5 –Loading actuators, measurement and vertical load

3. Test Results

The seismic load induces shear forces applying on the overall structural system, which consists of wing wall and frame components. Overall base shear force for each case can be calculated based on the forces of the loading actuators. Using the strain values of reinforcement to compute the shear forces of wing-walls for the corresponding cases. Table 1 presents the computed results of the each part of shear forces which indicate that wing walls sustain 92.5% of the overall base shear force, when subjected to small earthquakes. After the concrete cracks in the specimen under 1000 gal corresponding to the moderate earthquake, the stiffness degradation of wing walls occurs and the contribution of frame increases. This dual force-resisting mechanism demonstrates ductile behavior under seismic loads, because the damage of frames is postponed by the wing walls.

Table 1 – Scale factors of specimen compared to prototype structure

	Overall base shear force (kN)	Wing-wall shear force (kN)	Frame shear force (kN)
500 gal (small earthquake)	21.68	20.05（92.5%）	1.63（7.5%）
1000 gal (moderate earthquake)	104.81	88.35（84.3%）	16.46（15.7%）
2000 gal (large earthquake)	498.99	313.37（62.8%）	185.62（37.2%）
3000 gal (extra-large earthquake)	567.92	276.58（48.7%）	291.34（51.3%）

Fig. 6 shows the relationship curves between maximum roof drift ratio versus PGA of input earthquakes. The increasing of maximum rook drift ratio is nearly proportionate to the earthquake intensity. According to the values roof drift ratios in both direction, the laterial stiffnesses where the wing-walls in tension is slightly smaller than the oppsite side. Concrete Cracking at the bottom of the wing walls and yielding of the steel bars at the beam ends were the main reasons accounting for the stiffness reduction.

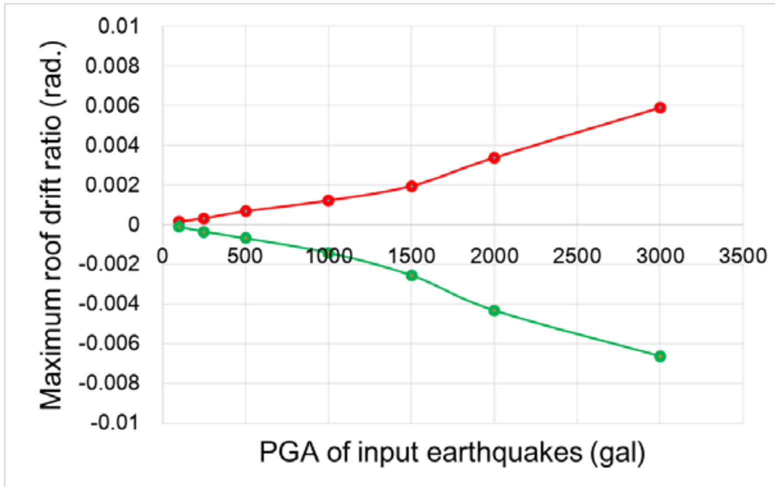

Fig. 6 – Relationship between maximum roof drift ratio versus PGA of input earthquakes

Hysteretic energy in structures is dissipated by generating plastic deformation and crack opening and closing. It indicates the extent of permanent damages remained after earthquakes. As for the pseudo-dynamic tests based on equivalent single-degree of freedom system, the damping energy can be neglected because the loading velocity in pseudo-dynamic test is very low. Thus, hysteretic energy account for a large percentage in the overall input energy.

The hysteretic plastic energy for each story level was calculated and normalized by the overall hysteretic energy to quantify the distribution and extent of plastic damages occurred. The hysteretic energy ratio is defined as the cumulative plastic energy absorbed by each primary story divided by the overall cumulative plastic energy as $\eta = W_{h,\,i}/\Sigma W_h$, where $W_{h,\,i}$ is the cumulative plastic energy absorbed by the i-th story; ΣW_h is the overall hysteretic plastic energy. Fig. 7 shows the ratio η of each primary story level subjected to 0.50, 1.00 and 2.00 g corresponding to the seismic criteria of Levels 1, 2 and 3. The first primary story (0.00 ~ 2.40 m) sustained 54.2, 50.8 and 46.1 % relative to the overall hysteretic energy respectively under the PGA of 0.50, 1.00 and 2.00 g. In contrast, the ratio η at the second primary story (2.40 ~ 4.80 m) significantly increased from 20.3 % to more than 43.9 % when the PGA was scaled from 0.50 to 2.00 g, and the top primary story (4.80 m ~ 7.20 m) sustained the smallest part of the ratio η.

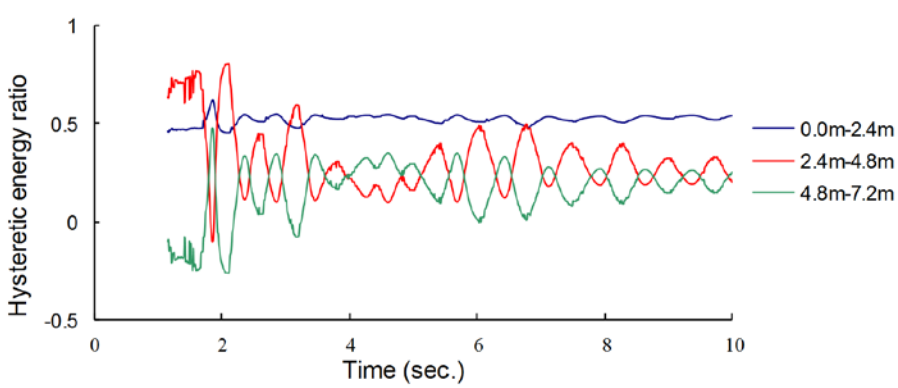

(a) Small earthquake in 8-degree seismic zone

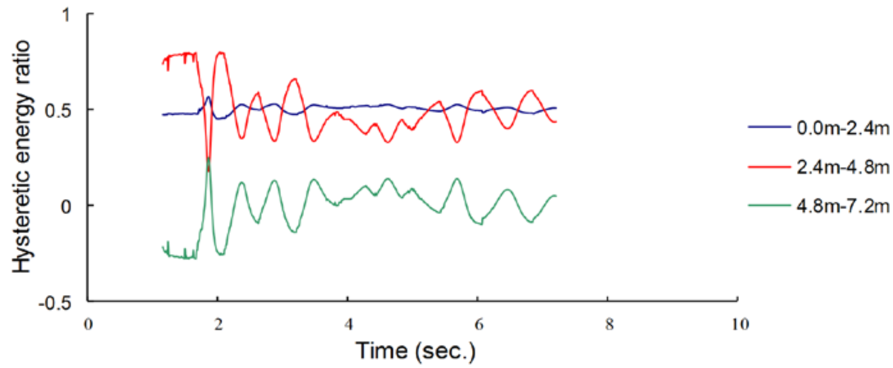

(a) Moderate earthquake in 8-degree seismic zone

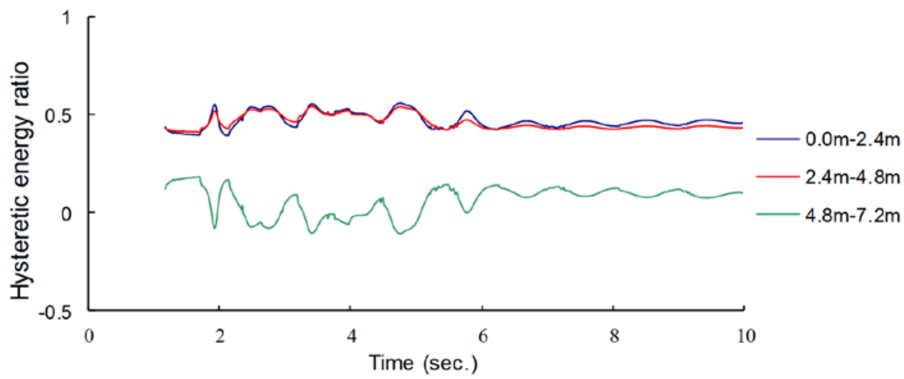

(a) Large earthquake in 8-degree seismic zone

Fig. 5 –Loading actuators, measurement and vertical load

4. Conclusions

This paper developed dual wing-walled frame system consists of irregular SRC frame with bi-directional RC wing walls. Through a series of pseudo-dynamic tests on a scaled steel-concrete moment frame with SRC columns and RC wing walls, the seismic behavior and failure mechanism have been investigated. The influences of TWW and LWW on the failure mechanisms of the wing-walled frame system have been discussed. The specimen demonstrated ductile behavior to resist severe earthquakes with PGA=3.0 g which is beyond the code requirement of PGA=3.0 g whose return period is 2 % in 50 years, whereas a region of drift concentration was found in the range of 2.40~4.80 m. Various primary story levels of the specimen showed difference in deterioration behavior, which is consistent with the contribution ratios of the cumulative hysteretic energy. The first and second primary stories dissipated most of the input hysteretic energy.

5. Acknowledgements

This paper is supported by the National Natural Science Foundation of China (NSFC) under Grant No. 51508459. This financial support is gratefully acknowledged.

6. References

[1] Hueste MBD, Wight JK (1997): Evaluation of a four story reinforced concrete building damaged during the Northridge earthquake. *Earthquake Spectra*, **13** (3), 387-414.

[2] Llera J, Chopra A, Almazán J (2001): Three-dimensional inelastic response of an RC building during the Northridge earthquake. *J. Struct. Eng.*, **127** (5): 482–489.

[3] Ivanović SS, Trifunac MD, Novikova EI, Gladkov AA, Todorovska MI (2000): Ambient vibration tests of a seven-story reinforced concrete building in Van Nuys, California, damaged by the 1994 Northridge Earthquake. *Soil Dynamics and Earthquake Engineering*, **19** (16): 391-411.

[4] Azizinamini A, Ghosh S (1997): Steel reinforced concrete structures in 1995 Hyogoken-Nanbuearthquake. *J. Struct. Eng.*, **123** (8): 986–992.

[5] Architectural Institute of Japan. 2012. Preliminary reconnaissance report on the 2011 Tohoku-Chiho Taiheiyo-Oki earthquake,AIJ. (in Japanese)

[6] Yamakawa T, Rahman MN, Morishita Y (2006): Experimental investigation and analytical approach for seismic retrofit of RC column with wing-wall. *J. Struct.& Const. Eng.,* **608**: 109-117.

[7] Kabeyasawa T, Kim Y, Mitsuharu S, Hyun SH, Yoji H (2011): Experimental study on deformability of RC columns with wingwall : Part 3 : Evaluation of deformability based on flexure theory. *Summaries of technical papers of annual meeting AIJ C-2*, **Structures IV**: 139-140.

[8] Nakamura A, Teshigawara M, Inoue Y, Ohta T (2011): Shear strength estimation of seismic retrofitted RC column by extended wing walls. *J. Struct. & Const. Eng.*, **76** (661): 619-627. (in Japanese)

[9] Liu K, Liu Y, Huang W, Chen C (2010): The structure behavior of reinforced concrete wing-wall under earthquake. *Int. J. of the Phy. Sci.*, **5** (7): 1164-1174.

[10] Higashi Y, Ohkubo M, Eto H (1970): Cracks and staticalhysteresis-loops of reinforced concrete frames with spandrel-walls cast simultaneously. *J. Struct. & Const. Eng.,* **169**: 1-8. (in Japanese)

[11] Kabeyasawa T, Kabeyasawa T, Matsumori T, Kim Y (2008): Full-scale dynamic collapse tests of three-story reinforced concrete buildings on flexible foundation at E-Defense. *14th World Conf. on Earth. Eng.*, Beijing, China.

[12] Kim Y, Kabeyasawa T, Matsumori T, Kabeyasawa T (2012): Numerical study of a full-scale six-story reinforced concrete wall-frame structure tested at E-Defense. *Earth. Eng. &Struct.Dyn.,* **41** (8): 1217-1239.

[13] Wallace J, Elwood K, Massone L (2008): Investigation of the axial load capacity for lightly reinforced wall piers. *J. Struct. Eng.*, **134** (9): 1548–1557.

[14] Bai Y, Bai G (2016): Pseudo-dynamic and quasi-static testing of an irregular steel concrete composite frame with wing walls. *International Journal of Structural Stability and Dynamics*, **16** (2): 1450095-1450120.